

PRECISE ORBIT DETERMINATION FOR GEOSAT FOLLOW-ON  
USING SATELLITE LASER RANGING DATA AND INTERMISSION ALTIMETER CROSSOVERS

Frank G. Lemoine, David D. Rowlands, Scott B. Luthcke  
Space Geodesy Branch, Code 926, NASA GSFC

Nikita P. Zelensky, Douglas S. Chinn, Despina E. Pavlis  
Raytheon ITSS Corp., Lanham, MD

Gregory C. Marr  
Flight Dynamics Analysis Branch, Code 572, NASA GSFC

**ABSTRACT**

*The U.S. Navy's GEOSAT Follow-On Spacecraft was launched on February 10, 1998 with the primary objective of the mission to map the oceans using a radar altimeter. Following an extensive set of calibration campaigns in 1999 and 2000, the US Navy formally accepted delivery of the satellite on November 29, 2000. Satellite laser ranging (SLR) and Doppler (Tranet-style) beacons track the spacecraft. Although limited amounts of GPS data were obtained, the primary mode of tracking remains satellite laser ranging. The GFO altimeter measurements are highly precise, with orbit error the largest component in the error budget. We have tuned the non-conservative force model for GFO and the gravity model using SLR, Doppler and altimeter crossover data sampled over one year. Gravity covariance projections to 70x70 show the radial orbit error on GEOSAT was reduced from 2.6 cm in EGM96 to 1.3 cm with the addition of SLR, GFO/GFO and TOPEX/GFO crossover data. Evaluation of the gravity fields using SLR and crossover data support the covariance projections and also show a dramatic reduction in geographically-correlated error for the tuned fields. In this paper, we report on progress in orbit determination for GFO using GFO/GFO and TOPEX/GFO altimeter crossovers. We will discuss improvements in satellite force modeling and orbit determination strategy, which allows reduction in GFO radial orbit error from 10-15cm to better than 5 cm.*

**INTRODUCTION**

The launch of the GEOSAT Follow-On (GFO) satellite February 10, 1998 marks the beginning of the Navy program to develop an operational series of low-cost altimeter satellites for maintaining continuous ocean observation via the GEOSAT exact repeat orbit (Table 1). GFO provides real-time measurements of the relative ocean heights for tactical applications and absolute heights post-processed for large-scale ocean modeling. Its inclination and ground-track repeat period serve to complement altimeter datasets collected by other missions such as TOPEX, ERS1 and ERS2.

GFO carries a single frequency (13.5 GHz) radar altimeter, a dual frequency water vapor radiometer, a dual frequency Doppler beacon for operational tracking, a laser retro reflector array (LRA) and four Global Positioning System (GPS) dual-frequency receivers for precision orbit determination (POD).

The measured quantity of interest, the ocean surface above the reference ellipsoid, is in fact a combination of two measurements: the ocean surface with respect to the satellite as observed by the altimeter, and the satellite height above the reference ellipsoid determined from the satellite tracking. GFO's capability to produce precise observations of the ocean surface thus depends critically on the accuracy of the orbits produced from the Doppler, SLR, or GPS tracking. GFO pre-launch analysis anticipates an accurate altimeter product (Table 2).

Since the GPS receivers delivered only limited data<sup>1</sup>, SLR tracking has provided the only means for computing highly accurate orbits, and has been designated as the primary tracking system for GFO POD. The 5-cm radial orbit error estimate for SLR tracking shown in Table 2 was derived in a pre-launch simulation study<sup>2</sup> It is the Root Mean Square (RMS) error over one day.

The Space Geodesy Branch at Goddard Space Flight Center (GSFC) has been given the task of improving GFO POD. This work has included pre-flight orbit error analysis, tuning a "macro-model" of the approximate spacecraft geometry and surface properties in order to better model the nonconservative forces, tuning the gravity model, computing the SLR based Medium Precision Ephemeris (MOE) on a daily basis for use on the NAVY NGDR and NOAA IGDR altimeter products, and providing the SLR based precise ephemeris (POE) for the CalVal evaluation efforts.

This paper reviews the analysis of GFO tracking data (SLR, Doppler, altimeter crossover) and tuning of the various models. Previously, using untuned models, GFO POD radial orbit accuracy was at the 10cm level<sup>3</sup>. Now, thanks to improved force modeling and the use of altimeter crossover data, GFO radial accuracy is believed to be below 5 cm.

## ORBIT MODELING AND ANTICIPATED ERRORS

Orbit determination can be stated as the adjustment of the orbit state, force, and measurement model parameters to minimize, in a least squares sense, the weighted difference between the actual tracking observations and their modeled values. The accuracy of the computed orbit depends on the accuracy and completeness of the force models, the measurement models, and the precision and coverage of the tracking data. GEODYN<sup>4</sup>, a state-of-the-art least squares orbit determination and geodetic parameter recovery program, developed and maintained at GSFC, is used for GFO POD. Table 3 shows a summary of the POD models.

Several gravity fields were tested, EGM96<sup>5</sup>, TEG3<sup>6</sup>, JGM3<sup>7</sup>, and PGS7609G, a GSFC combination model based on EGM96 but with additional TDRSS satellite tracking data from the EUVE, ERBS, XTE, GRO, and TRMM satellites. PGS7728 and PGS7727 are two preliminary fields, tuned using PGS7609G and GFO SLR, Doppler, and GFO/GFO altimeter crossover data. In addition to the data used for PGS7728, TOPEX/GFO crossover data was also used to tune PGS7727. Although covariance projections indicate that orbit error due to gravity will be only 1-3 cm (Table 4), the error structure will be complex, and include a geographically correlated component. By spherical harmonic order, the radial orbit error due to gravity is highest at order 1, and in the vicinity of the k=2 resonance (near order 29) (Figure 1). Tuning with GFO tracking data reduces this error

Nonconservative forces acting on GFO consist of radiative forces and atmospheric drag. Radiative forces include solar radiation pressure, the Earth's albedo (reflected light) and infrared radiation, and other secondary effects such as thermal imbalance in emission from spacecraft surfaces. Secondary effects are not modeled for GFO. The macro-model approximates GFO's surface geometry and material properties using eight plates (Figure 2). Each plate has been assigned a body-fixed orientation, area, and specular and diffuse reflectivity coefficients based on pre-launch engineering information. All plate interaction effects, such as self-shadowing and multiple reflections, are ignored. The total acceleration with respect to the center of mass (CoM) is computed by summing vectorially the force acting on each plate, taking into account each plate's area, angle of incidence and material properties. Throughout the orbit and over a Beta prime cycle, radiation will be incident to a changing orientation of the macro-model as computed using an analytical attitude model. Beta prime is the angle to the sun from the orbit plane (Figure 3), and for GFO shows a period of about 336 days.

As shown in Figure 4, the largest nonconservative force acting on GFO is by far due to solar radiation pressure. Since the solar radiation pressure is so large, even a small error will have a significant impact. The error for the macro-model should be 10 to 20 percent of the radiative force. For instance, the *a priori* macro-model for TOPEX was meticulously constructed using finite element modeling and could only account for 90% of the radiative forces<sup>8</sup>. However, after tuning, the TOPEX macro-model is believed to account for over 95% of the radiative forces<sup>9</sup>. The approach taken for the *a priori* GFO macro-model construction was much simpler and without application of finite element modeling. Even a 5% mismodeling of the solar radiation pressure would constitute a considerable source of error, requiring the adjustment of sufficient empirical acceleration parameters for reducing orbit error to an acceptable level for POD<sup>10</sup>. It has been shown in a previous study (Ref. 3) that given the 1999 level of SLR tracking, orbit error is due primarily to mismodeling of the radiative forces acting on the satellite. The same study (Ref. 3) also shows that following adjustment of the LRA offset to spacecraft Center of Mass (CoM), all error in the SLR measurement modeling remains very small including error in the analytical attitude model.

## TRACKING DATA AND POD STRATEGY

GFO POD relies on SLR tracking provided by a global network of NASA and foreign stations (Figure 5). Operational tracking Doppler data from the three stations (Guam; Point Mugu, California; and Prospect Harbor, Maine) although noisy (2 cm/sec) is abundant, and serves to slightly strengthen the SLR solution. After 40% of the data is edited, typically nine Doppler passes per day remain. The Doppler station positions have been adjusted to the SLR frame using three months of Doppler data and SLR-determined orbits that were held fixed in the solution.

The recent increase in SLR tracking has been very welcome news for GFO POD, growing from an average of 7 passes/day for 1998 and 1999 to over 9 passes /day for 2000 and 2001. The 33% increase in tracking for 2000 is accompanied by a 22% increase in the number of tracking stations (see Table 5 and Figure 5). The long awaited site at Hartebeesthoek, South Africa, became operational late last year, 2000. This new NASA site, an important addition to the SLR Network, brings better balance to the North – South tracking distribution.

Given the SLR tracking density, an arc length of five days was selected over shorter arcs to increase the dynamic strength of the solution<sup>i</sup>. Arc lengths of nine and ten days would also be suitable, however the frequency of satellite events over 1998 and 1999, such as computer resets or maneuvers which are not modeled for POD, have allowed only a few uninterrupted ten day spans.

Altimeter crossover data, computed by differencing altimeter ranges from two intersecting passes interpolated to a common geographic point, can be used to supplement the SLR and Doppler data for POD. Continuous altimeter tracking only began in mid-December '99. GFO crossovers provide dense spatial coverage and promise a high accuracy product<sup>ii</sup>. Crossovers used in POD are edited in regions which have high sea surface variability (greater than 20cm) and in shallow seas (1000m or less). It is possible to combine GFO with TOPEX altimeter data to form TOPEX/GFO altimeter crossover data (Table 6). From the well-defined and accurate TOPEX reference it may be possible to better calibrate the GFO altimeter corrections, to better tune the GFO macro-model and gravity field, and to better determine GFO orbits. The effective use of intermission altimeter crossover data to improve POD has been demonstrated for the ERS-1 and ERS-2 satellites<sup>11</sup>. In the very least, the quantity of crossover data is increased 3-fold with the addition of TOPEX/GFO crossovers, further strengthening the orbit solution.

The solution strategy, with the objective to minimize orbit error, was developed considering the strength of the tracking data. Several parameterization schemes were tested and the one finally selected for SLR is summarized in Table 3. According to this strategy orbit error is minimized by adjusting, in addition to the orbit state, atmospheric drag scale coefficients and empirical one cycle per revolution (1cpr) accelerations for both the along-track and cross-track components. The empirical and drag terms can absorb much of the residual accelerations which remain from the mismodeling of the various forces, and greatly reduce orbit error<sup>12, 13</sup>. With perfect tracking data, adjustment of empirical accelerations can remove all orbit error with a sufficiently dense time series of the adjusted parameters. Imperfection in data and coverage limit the capability of empirical acceleration parameters to remove orbit error. Since the adjusted empirical acceleration terms capture information about the residual accelerations, they can also reveal characteristics of the mismodeled forces.

Sparse SLR tracking restricts the number of empirical accelerations which can be adjusted in the orbit solution, thereby limiting the capability for removing these residual accelerations. Including altimeter crossover data significantly strengthens the solution and can lead to far better orbits (Figure 6), however the GFO crossover data should be used with caution. It is believed about 40%-60% of the highly variable ionosphere refraction effect is not removed from the altimeter data with the IRI95 model. The ionosphere exhibits a high/low day/night effect. Since the GFO groundtrack repeats every 17 days and 15 minutes, the local time for a given pass will only advance by 15 minutes every 17 days. In our tests using July '99 data nearly all descending passes occurred during the day. Thus over extended periods the residual ionosphere day/night (descending pass / ascending pass) effect will directly contribute to a once per orbit revolution error (1/rev) when crossovers are used in the solution (Table 7). Nonetheless the orbit improvement gained appears to overshadow any orbit error induced with the use of crossover data (Figure 6). Thus including crossover data allows the adjustment of more empirical parameters to better remove non-conservative force model error. It is important to note that for solutions which include and which do not include crossover data, orbit accuracy remains correlated to the number of SLR points present (Figure 7). In the combination solution the presence of SLR data probably acts to constrain the effect of the ionosphere error contained in the GFO altimeter crossovers.

No single test can uniquely gauge orbit accuracy. This analysis uses SLR residuals, or the misclosure between the highly precise observed and computed ranges, altimeter crossover differences in which the non-orbit signal is believed to dominate (Table 8), and orbit differences between arcs sharing one day of overlapping data, to indicate the level of orbit error. Overlap orbit differences identify the least amount of orbit error shared by the two arcs across the overlap period, as common errors will cancel. Altimeter crossover differences represent the time-varying error component of both the altimeter measurement and orbit, as geographically correlated error is cancelled. Thus GFO/GFO crossover differences do not contain geographically correlated orbit error, but the TOPEX/GFO crossovers differences are expected to contain such orbit error for both satellites, as geographically correlated orbit error varies with satellite altitude. Since TOPEX orbit error is believed to be small, it is anticipated that TOPEX-GFO crossover data will be very useful for tuning the gravity field and gauging geographically correlated error for GFO. The GFO altimeter crossover non-orbit component estimate of 5.5 cm (Table 8) was actually derived from several tests using both GFO and TOPEX altimeter crossover data. The "non-orbit" is that component of the crossover signal, which could not be absorbed by the adjustment

---

i. In cases of sparse tracking one can usually rely on the fidelity of the dynamic force models to determine a better orbit over a longer span. Over a shorter arc, the solution may be ill determined, and the orbit error very large over periods with no data.

ii GFO IGDR altimeter data obtained from John Lillibridge, NOAA.

of any number of orbit parameters and must be due to ocean variability, residual ionosphere and altimeter noise. The TOPEX altimeter crossover non-orbit signal was estimated to be 4.9 cm.

## MACRO-MODEL TUNING

The macro-model represents the GFO spacecraft as an eight surface composite (Figure 2). It approximates the spacecraft geometry and surface material properties to better model the surface force effects due to solar and terrestrial radiation pressure, and due to atmospheric drag. Each surface (or plate) had been assigned an orientation with respect to the satellite fixed frame, an area, and a specular and diffuse reflectivity coefficient based on pre-launch engineering specifications. The material properties of each plate are assumed to be homogenous, representing an average value. In tuning, these average values are adjusted to best fit the GFO tracking data using an orbit determination (OD) solution strategy to insure the mismodeled nonconservative forces are not absorbed in empirical parameter adjustments. Therefore the macro-model is tuned to the residual satellite acceleration history which is based on orbit errors sensed from the spacecraft tracking data.

OD parameterization suitable for macro-model tuning adjusts the orbit state, and one drag coefficient ( $C_D$ ). The solar radiation pressure coefficient ( $C_R$ ), which should remain constant, is fixed to a value of 1.0. Upon solution convergence, GEODYN writes out the normal equations for the orbit (state,  $C_D$ ) and panel (area, specular, diffuse) parameters for each arc. These normal equations were combined from arcs sampled over the Beta prime cycle and the selected panel parameters estimated using Bayesian least squares. A preliminary sensitivity study was performed using the combined normal matrix from four well-spaced arcs to help identify panel parameters that were to be estimated. Assuming a specified allowed percent change in each respective panel parameter *a priori* value, and using only the left-hand side diagonal (variance) terms of the normal matrix, the resulting "uncorrelated weighted variance" is computed in order to compare parameter sensitivity, or change in residual variance, with respect to parameter adjustments. The *a priori* surface area assigned to each plate is believed to be relatively well determined with about a 10% error. There is much greater uncertainty for the *a priori* specular and diffuse reflectivity coefficients, computed as an aggregate average of these properties for each surface. The area is allowed to change by 10% and the reflectivity coefficients by 100% for the sensitivity analysis. As shown in Figure 8, specular coefficients for four parameters representing the solar array, the bottom plate (+z facing Earth), and the top and bottom sides of the altimeter antenna reflector, are likely candidates for the macro-model tuning adjustment.

The solar array specular reflectivity coefficient was adjusted using 31 SLR+Doppler arcs, 8 of which include Crossover data, spanning over 20 months (May 22, 1998 to February 6, 2000) or well over the 336 day Beta prime period. The preliminary tuned macro-model shows improvement in SLR fits, even for solutions adjusting empirical parameters (Table 9). Note that the *a priori* macro-model also shows improvement over the "cannonball" or spherical model, which would have been used in the absence of a macro-model (Table 9).

Even though the tuned macro-model shows improvement in SLR fits, the recovered empirical acceleration amplitudes and phases (Figures 9 and 10) are strongly correlated with Beta prime. This indicates that the solar radiation pressure still remains the largest mismodeled force, and that further tuning may be warranted.

As the absolute value of Beta prime increases from zero to 80+ degrees the solar radiation pressure (and the mismodeled effect) will change its projection from predominately along-track and radial directions to cross-track (Figure 4). The adjusted empirical accelerations should thus decrease in magnitude in the along-track component (Figures 9 and 10), and increase in the cross-track. The associated phase (with respect to orbit angle) will remain constant from arc to arc until the spacecraft enters the full sunlight regime. The observed phase coherence (Figure 10) indicates that the force error preserves the same orientation with respect to orbit plane from arc to arc, which in fact solar radiation pressure does. As the spacecraft reaches full sunlight (near  $|65^\circ|$  Beta prime), the recovered along-track acceleration magnitude becomes very small and for which the phase is not well determined. The along-track acceleration changes phase between increasing/decreasing Beta prime (Figure 10). In another study tuning the TDRSS macro-model<sup>14</sup>, a continuous phase was also observed in the recovered 1cpr along-track acceleration prior to tuning. After tuning, the recovered acceleration magnitudes were small and the phases showed no coherence.

## GRAVITY MODEL TUNING

Two preliminary gravity models were determined using SLR, Doppler, and GFO/GFO and TOPEX/GFO altimeter crossover data. Twenty arcs spanning one year from June 1999 to June of 2000 were included, whose arc length ranged from two to ten days (the average arc length was 6.8 days). An average of 5967 TOPEX/GFO altimeter crossovers and 2728 GFO/GFO altimeter were included in each arc. The average RMS of fit over these 20 arcs prior to gravity tuning was 7.07 cm for the TOPEX/GFO crossover data, 7.71 cm for the GFO/GFO crossover data, and 5.68 cm for the SLR data. In the solution derivation, the TOPEX

orbit was first determined using SLR and DORIS data, and then held fixed in both the GFO orbit adjustment and gravity field tuning. Two solutions were estimated: PGS7728, which included the GFO SLR, Doppler and GFO/GFO altimeter crossover data, and PGS7727, which included these data, as well as the TOPEX/GFO crossover data. The entire set of GFO data was calibrated using the Lerch method of subset calibrations<sup>15</sup>. An overall calibration factor of 0.78 was obtained, indicating the data were conservatively weighted in the tuned solutions. The radial orbit error due to the geopotential projected from the two new solutions to 70x70 show a significant improvement in orbit accuracy, particularly at order 1, and near order 29 (see Figure 1). The total predicted radial orbit error due to the geopotential on the GFO orbit is 1.31 cm with PGS7727. Looking at several gravity fields, the SLR and crossover data RMS of fit for several test arcs, show a marked improvement for the tuned fields (Table 10)

Since the TOPEX geographically correlated orbit error is believed to be less than 1 cm (Ref. 10), it may be possible to differentiate the GFO geographically correlated error by geographically projecting the TOPEX-GFO altimeter crossover residuals. Indeed, after averaging crossover residuals from five 10-day arcs over 5° x 5° bins, geographic structure becomes apparent for PGS7609G and to a lesser degree for PGS7728 and PGS7727 (Figure 12). Note the large peak-to-peak amplitude of ± 8 cm for the C(2,2) type signal present for PGS7609G, is progressively reduced to a peak-to-peak amplitude of only ± 3 cm. The introduction of the TOPEX/GFO altimeter data appears to have largely removed this C(2,2) effect. Orbit difference projections with respect to PGS7727 orbits (Figure 11) correspond to the improvements shown with the TOPEX-GFO crossover differences (Figure 12). Notice the difference in scale for Figure 11a and Figure 11b. Figure 12 illustrates a significant reduction in geographically correlated orbit error. It is likely that the geographically correlated error for PGS7727 is indeed close to 1 cm (Table 4).

Orbit error can be estimated from altimeter crossover fits. For example, PGS7727 shows a GFO crossover fit of 7.6 cm (Table 10). Assuming 5.5 cm of this signal is not due to orbit error (Table 8), leaves 5.2 cm representing the time-varying orbit error combined from the ascending and descending pass differences. Assuming the time-varying error is evenly distributed between ascending and descending passes and assuming a geographically correlated error component (1.2 cm for PGS7727 from Table 4) will give us a total radial error estimate:

$$\text{radial error estimate using crossovers} = \sqrt{(\text{crossover}^2 - \text{non\_orbit}^2)/2 + \text{geographically\_correlated}^2} \quad (1)$$

where

<i>crossover</i>	is the total altimeter crossover difference RMS value
<i>non_orbit</i>	is the non-orbit component of the altimeter crossover difference value
<i>geographically_correlated</i>	is the geographically correlated radial orbit error

Thus from the GFO crossover fit one may estimate PGS7727 orbits have a radial error of 3.9 cm, and that the orbit error probably remains dominated by non-conservative force mismodeling (Table 4).

## REDUCED DYNAMIC APPROACH

POD can benefit from the spatially dense altimeter crossover coverage by adjusting more empirical parameters. According to perturbation theory, most orbit error due to force mismodeling is of a resonant nature. The linearized equations of satellite motion, Hill's equations, further suggest that the orbit acts as a narrow bandwidth filter, smoothing the effects of complex acceleration perturbations, and that with the adjustment of nine parameters ( $A_R, B_R, C_R, A_L, B_L, C_L, A_C, B_C, C_C$ ) together with the state, orbit error will be dramatically reduced (Ref 12, 13).

Acceleration <sub>R</sub>	=	$A_R \cos(\omega t) + B_R \sin(\omega t) + C_R$	(Radial)
Acceleration <sub>L</sub>	=	$A_L \cos(\omega t) + B_L \sin(\omega t) + C_L$	(Along-track)
Acceleration <sub>C</sub>	=	$A_C \cos(\omega t) + B_C \sin(\omega t) + C_C$	(Cross-track)

or      Acceleration      =      Amplitude  $\cos(\omega t + \text{phase}) + \text{Constant}$

where

A's and B's	represent the adjusted Sine and Cosine amplitude terms (or 1cpr acceleration amplitude / phase terms)
C's	represent the adjusted constant acceleration terms
$\omega$	is the orbital frequency
t	is the time.

Our dynamic solution strategy calls for the adjustment of four parameters - the along-track and cross-track 1cpr terms. GFO tracking data cannot support the adjustment of Hill's entire set of nine empirical parameters. Even the adjustment of the four 1cpr

parameters over an arc dramatically reduces orbit error to the decimeter level (MOE dynamic strategy). At the 10-cm level, orbit error will largely consist of 1/rev terms and include the non-resonant terms. With the inclusion of altimeter crossover data it becomes possible to adjust the 1cpr acceleration parameters more frequently - over each day of the arc. This will further remove 1cpr orbit error as well as some daily and modulated signals, reducing the radial error to about 5-cm (POE dynamic strategy).

Our "reduced dynamic" approach, can reduce all orbit error signal, by allowing a more frequent adjustment of the 1cpr acceleration amplitude and phase parameters, roughly approximating a time varying empirical acceleration of the form:

$$\text{Acceleration}(t) = \text{Amplitude}(t) \cos(\omega t + \text{phase}(t))$$

Deficiencies in the tracking data are accommodated by suitably constraining the parameter adjustments. The success of a reduced dynamic approach depends on precision and density of the tracking data and on the accuracy of the dynamic force models, especially the gravity field. The GEODYN "reduced dynamic" implementation has been shown to improve the Space Shuttle precision orbit<sup>16</sup>. A subset of the GEODYN implementation is through the least-squares adjustment of a time series of 1cpr empirical acceleration parameters, which have explicitly correlated constraining equations forcing greater continuity between the adjacent 1cpr amplitude and phase terms. For any one such parameter  $P_j$ , the closer in time it is to another parameter  $P_k$ , the tighter is the constraint forcing both  $P_j$  and  $P_k$  to adjust to the same value. The weight used in the constraint equation between two parameters at time  $T_j$  and at time  $T_k$ , is computed in GEODYN as follows:

$$\text{weight}(j,k) = (e/\sigma^2) e^{-(|T_j - T_k|/\text{correlation time})}$$

where

- $T_j$  is the the mid-point of the jth acceleration parameter interval
- $\sigma$  is the process noise input by user
- correlation time is the correlation time input by user
- $e$  is the base of the natural logarithms (2.718 ...)

The acceleration parameter interval, correlation time, and sigma, selected from preliminary empirical tests (tuning), are 25 minutes, 12.5 minutes, and  $1.e-9 \text{ m/s}^2$  respectfully. Such a reduced dynamic approach processing SLR, Doppler and GFO/GFO crossover data offers some improvement over the standard dynamic approach (Table 11). The improvement is especially significant for the cross-track and along-track components as evidenced by the improved orbit overlap consistency (Table 11). Orbit error cannot be less than the orbit overlap differences, which indicate the radial error cannot be less than 1.7 cm. From the GFO crossover fits (Table 11), a radial error of 4.7 cm for the dynamic and 4.2 cm for the reduced-dynamic solutions, is estimated (Equation 1).

In these tests the TOPEX/GFO crossovers are used as independent data to measure the orbit accuracy. Radial orbit error may be estimated from TOPEX/GFO crossovers once the magnitude of the altimeter+TOPEX orbit component is identified in the crossover fits. Using a high and a low estimate for this component (Table 12), GFO radial orbit error is estimated to be between 4.6 cm – 5.6 cm. for the dynamic (7.9 cm crossover RMS from Table 11) and between 4.3 cm – 5.3 cm for the reduced dynamic solutions (Table 11). From these tests it appears that altimeter crossover data constrain the radial orbit component quite well for the dynamic solutions. However the dynamic orbit retains significant nonconservative force model error. This error may be further reduced with a reduced-dynamic strategy given adequate tracking. POD may be further improved with the inclusion of TOPEX/GFO crossover data, and with the application of other "tuning" combinations.

## SUMMARY

The Space Geodesy Branch at Goddard Space Flight Center (GSFC) has been given the task of improving GFO precision orbit determination. Since GPS receivers delivered only very limited tracking data, SLR tracking offers the only means with which to compute precise orbits for this spacecraft. SLR data in combination with altimeter crossover data was successfully used to tune the preliminary macro-model and gravity field. Use of intermission altimeter crossover data (TOPEX/GFO) significantly contributed to reducing geographically correlated error for the tuned gravity field. The radial orbit accuracy is estimated to be 4-5 cm using the latest models and including altimeter crossover data in the orbit solution.

With the termination of the CalVal phase, better altimeter corrections have become available which will favorably impact the GFO orbit determination. For example, the estimate of the sea state (EM) bias has been refined, and the wet troposphere correction from the on-board radiometer has been validated. In addition, improved tidal solutions have been derived primarily from TOPEX altimeter data (eg GOT00.2) and will be applied in future work. Use of TOPEX/GFO crossover data is anticipated to further help GFO macromodel tuning and, in combination with the reduced-dynamic approach, to further help GFO precision orbit determination. Future work should include a review of the nonconservative force model, and whether more detailed modeling is warranted, as for example including shadowing and thermal radiation effects.

## TABLES AND FIGURES

**Table 1 GEOSAT Exact Repeat Orbit**

Orbit parameter	value
Altitude	800 km
Eccentricity	0.0008
Inclination	108 deg
Repeat Period	244 revs in 17 days

**Table 2 GFO Pre-Launch Altimeter Error Budget<sup>iii</sup>**

Component	Source	Error (cm)
Altimeter		
instrument noise	Ball	1.9
biases	Ball	3.0
sea surface (EM & skewness)	TOPEX	2.3
Media		
troposphere	Ball	2.0
ionosphere	Ball	1.7
SLR POD (radial orbit)	GSFC	5.0
Total RSS		7.1

**Table 3 GFO Precise Orbit Determination Modeling**

Model Category	Description
Geophysical models Gravity Ocean/Earth Tides Atmospheric density Spacecraft geometry and surface forces Station Coordinates Earth Orientation Parameters Planetary Ephemeris	PGS7727 (PGS7609G + GFO SLR, Altimeter Crossover, and Doppler tracking data) PGS7723C <sup>i</sup> resonant + Ray '99 background terms <sup>17</sup> MSIS-86 <sup>18</sup> GFO Preliminary tuned macro-model CSR95L02 SLR solution frame <sup>ii</sup> CSR95L02 from LAGEOS tracking DE403
Measurement Model SLR Doppler Altimeter Crossover	<i>A priori</i> CoM, estimated LRA offset, analytical attitude <i>A priori</i> CoM, <i>a priori</i> beacon offset, analytical attitude <i>A priori</i> CoM, analytical attitude, GEODYN Dynamic Crossover model
Tracking Data Weights SLR Doppler Altimeter Crossover	10 cm 2 cm/sec 10 cm
Estimated Parameters	Orbit state, Atmospheric drag $C_D$ per day (or more frequently data permitting) Along-track 1cpr empirical acceleration per arc Cross-track 1cpr empirical acceleration per arc Doppler measurement and troposphere bias per pass

<sup>i</sup> PGS7723C is a preliminary field determined from PGS7609G + GFO SLR/Doppler and GFO/GFO Altimeter Crossover data.

ii. CSR95L02 is the SLR station position and velocity frame used to compute the TOPEX/POSEIDON precise orbits, Richard Eanes, CSR, 1995.

iii. An official GFO altimeter system error budget has yet to be published. The values shown here have been compiled from an internal Ball document provided by Scott Mitchell, from the T/P Mission Plan, and error simulations performed at GSFC (Ref 2).

**Table 4. Gravity Orbit Error Covariance (to 70x70) Projection**

Gravity Field	GFO Orbit Error (cm)			
	geographically correlated Radial	Radial	Cross-Track	Along-Track
JGM3	4.53	4.97	23.80	42.61
TEG3	3.30	3.48	21.42	42.76
EGM96	2.35	2.61	8.94	17.72
PGS7609G	2.35	2.61	8.93	16.44
PGS7728	1.49	1.66	8.57	14.84
PGS7727	1.16	1.31	8.42	14.40

**Table 5. SLR Tracking Summary**

Year	Days	Stations	Passes
1998	254	33	1829
1999	365	32	2625
2000	366	39	3485
2001	59	27	543

**Table 6. Altimeter Range Modeling for TOPEX/GFO Crossover Processing**

Model	TOPEX <sup>i</sup>	GFO <sup>ii</sup>
Ocean tide + tidal loading	CSR 3.0 (GDR)	same (IGDR)
Earth Tide	Cartwright (GDR)	same (IGDR)
Dry troposphere	FMO (GDR)	NCEP (IGDR)
Wet troposphere	TMR (GDR)	NCEP <sup>iii</sup> (IGDR)
Ionosphere	dual frequency (GDR)	IRI95 (IGDR)
Inverse barometer	$f$ (dry troposphere)	same $f$ function
EM bias	Walsh (GDR)	5% SWH
Orbit	fixed <sup>iv</sup>	adjusted
Range bias	fixed <sup>v</sup>	adjusted
Timing bias	fixed (GDR time tag)	adjusted

**Table 7. POD Sensitivity to Altimeter Ionosphere Error (July 28 – August 6 1999 data)**

Satellite and (Beta prime angle) <sup>a</sup>	ionosphere altimeter correction	SLR + Doppler Orbit held fixed		SLR+Doppler+altimeter crossover Orbit adjusted	
		crossover rms (cm)	variance reduction (cm <sup>2</sup> )	crossover rms (cm)	radial orbit difference(cm)
TOPEX (-30 °)	none	7.46		6.75	
	measured	5.97	20.00	5.77	1.50
GFO (-73 °)	none	9.04		6.81	
	IRI95	8.80	4.28	6.75	0.82

a) the largest ionosphere corrections are anticipated for Beta prime close to zero

<sup>i</sup> TOPEX GDR

<sup>ii</sup> GFO IGDR from NOAA

<sup>iii</sup> TMR value also available

<sup>iv</sup> POE has 2-3 cm radial accuracy

<sup>v</sup> routinely computed per cycle by PODPS based on the POE orbit

**Table 8. GFO/GFO Altimeter Crossover Error Budget**

Error Source	time varying error (cm)	
	range	crossover difference
Non-orbit altimeter	3.5	5.0
ionosphere	1.7	2.4
Orbit	3.7	5.2
RSS total		7.6

**Table 9. GFO Macro model Tuning**

spacecraft surface model	solar array (SA) reflectivity coefficient	SLR fits over 23 dependant arcs (cm)	SLR fits over 57 independent arcs (cm)	SLR fits over 80 arcs total <sup>b</sup> (cm)
cannonball	----	13.23	12.88	12.99
a-priori macro model	.160	13.11	12.89	12.95
tuned SA macro model <sup>a</sup>	.144	13.04	12.80	12.87

a) tuned using 23 SLR+Doppler and 8 SLR+Doppler +Crossover arcs spanning 980522 – 000206

b) 80 consecutive arcs spanning 980422 – 990603

**Table 10. Gravity Field Tests**

gravity field	radial orbit error projected from 70x70 gravity covariance (cm)	data RMS (cm) combined results over five 10-day arcs			
		TP crossover	TP/GFO crossover	GFO crossover	GFO SLR
JGM3	4.97	6.17	8.45	8.51	7.42
TEG3	3.48	6.20	7.31	7.95	6.89
EGM96	2.61	6.14	7.71	8.27	6.97
PGS7609G	2.61	6.16	7.74	8.26	6.75
PGS7728	1.66	6.14	7.17	7.68	5.64
PGS7727	1.31	6.13	7.02	7.59	5.53

**Table 11. GFO Orbit Solution Strategy**

Solution Strategy	TOPEX/GFO Crossover RMS (cm) (independent data)	GFO tracking data RMS <i>combined results over seven 5-day arcs (Jan 17 '00 – Feb 13 '00)</i>			orbit overlap difference RMS (cm)		
		Doppler (cm/sec)	SLR (cm)	GFO Crossover (cm)	radial	cross track	along track
moe (dynamic) 1 drag/24 hours, 1 cpr/5 days	11.2	2.1	31.1	12.8	6.7	23.0	83.0
poe (dynamic) 1 drag/08 hours, 1 cpr/1 days	7.9	2.0	5.2	8.5	2.3	24.5	23.2
reduced dynamic 1 drag/24 hours, 1 cpr/25 min	7.7	2.0	4.1	7.9	2.4	9.0	16.1

**Table 12. TOPEX/GFO Altimeter Crossover Error Budget**

Error Source	High GFO orbit estimate (cm)			Low GFO orbit estimate (cm)		
	TP range	GFO range	crossover	TP range	GFO range	crossover
altimeter time varying	3.5	3.5	4.9	3.5	3.5	4.9
ionosphere	0	1.7 <sup>a</sup>	1.7	0	2.8 <sup>b</sup>	2.8
orbit	2.0	5.3	5.7	3.0	4.3	5.2
RSS total	7.7			7.7		
RSS altimeter + TP orbit	5.6			6.4		

a. Ball estimate

b. RSS difference( measured ionosphere for TP – IRI95 modeled for GFO; see Table 7)

**Figure 1. GFO Gravity Orbit Error Covariance (to 70x70) Projection**

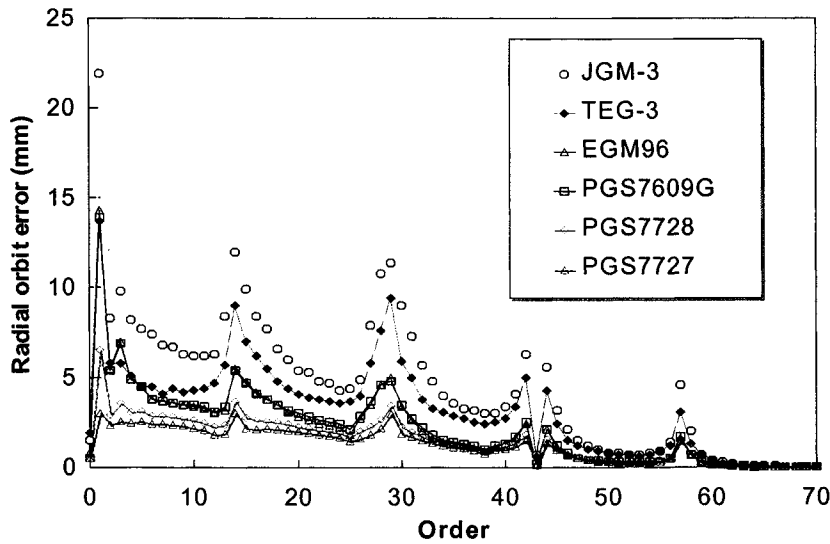
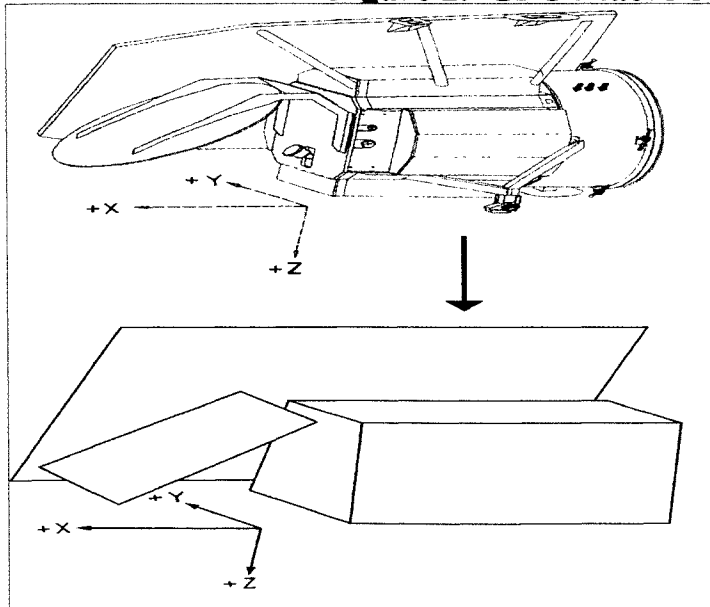


**Figure 2. GFO Macro-Model Approximation**



Acceleration due to radiation pressure on a flat plate:

$$\Gamma = -\frac{\Phi A \cos \theta}{Mc} [2(\delta/3 + \rho \cos \theta) \mathbf{n} + (1 - \rho) \mathbf{s}]$$

where

- $\Gamma$  = acceleration (m/s<sup>2</sup>)
- $\Phi$  = radiation flux from source
- $A$  = surface area of flat plate (m<sup>2</sup>) \*
- $\theta$  = incidence angle
- $M$  = satellite mass (m)
- $c$  = speed of light (m/s)
- $\delta$  = diffuse reflectivity \*
- $\rho$  = specular reflectivity \*
- $\mathbf{n}$  = surface normal unit vector
- $\mathbf{s}$  = source incidence unit vector

\* are the adjustable macro model parameters

**Figure 3. Orbit geometry**

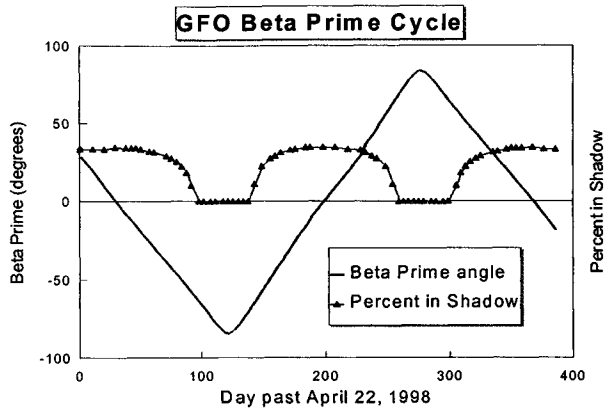
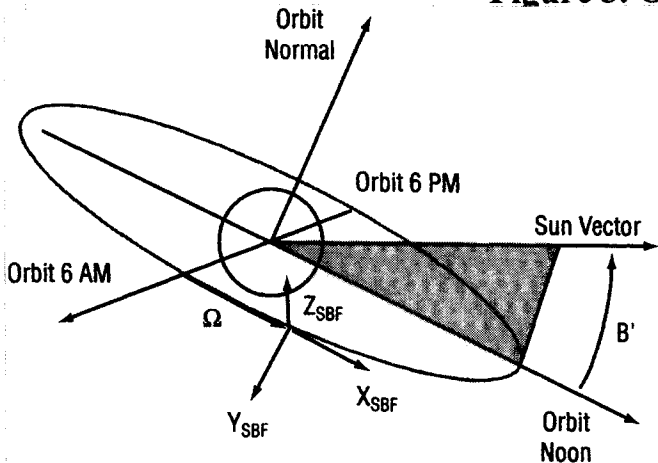


**Figure 4. Non-conservative forces acting on GFO**

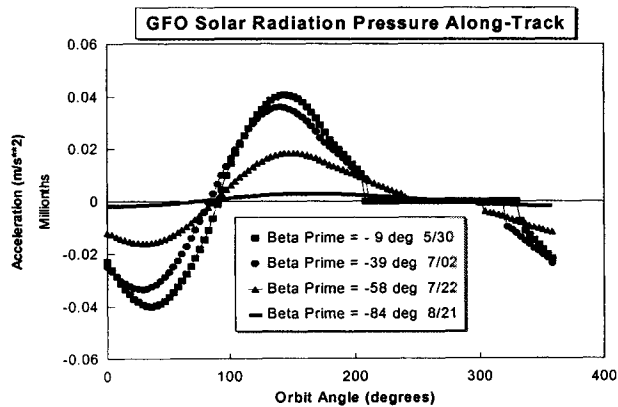
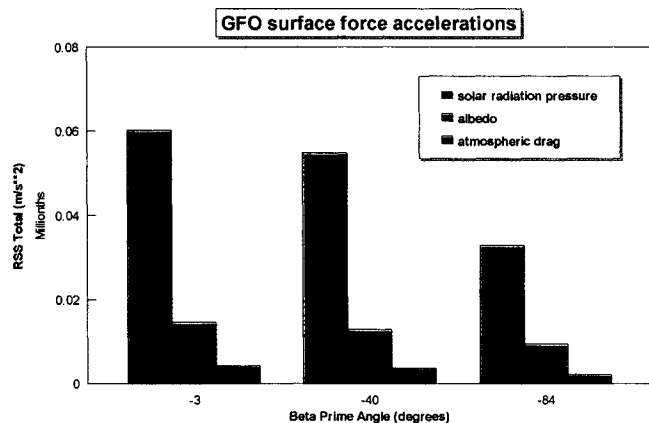
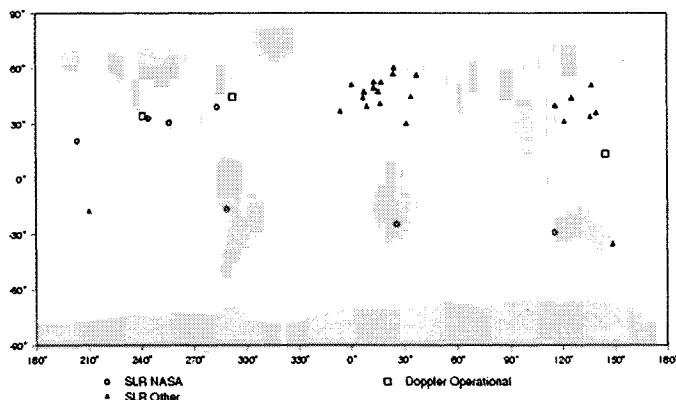


**Figure 5. GFO Tracking Network**



**GFO SLR Tracking History**

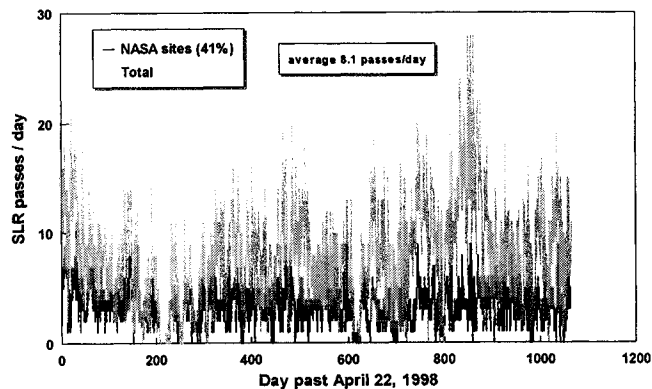


**Figure 6. GFO Orbit Solution Strategies**  
*nominal: 1drag/day, 1crp/5day; enhanced: 3drag/day, 1crp/1day*  
**Combined nine arcs spanning Jan 6 –Feb 13 2000**

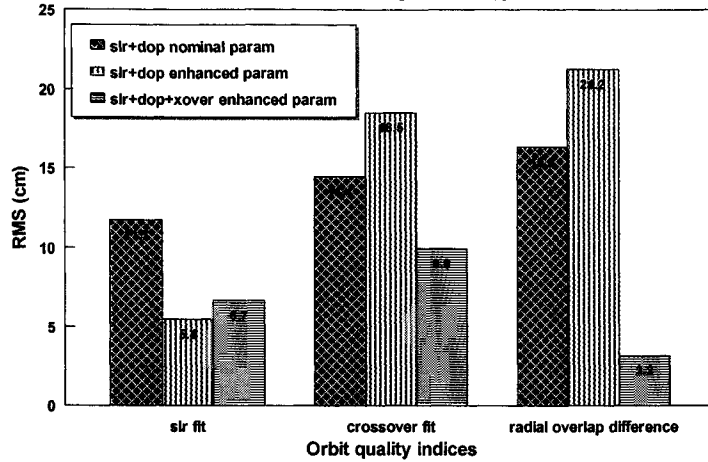


**Figure 7. Orbit accuracy limited by sparse SLR tracking**  
*GFO-GFO Altimeter Crossover Differences*

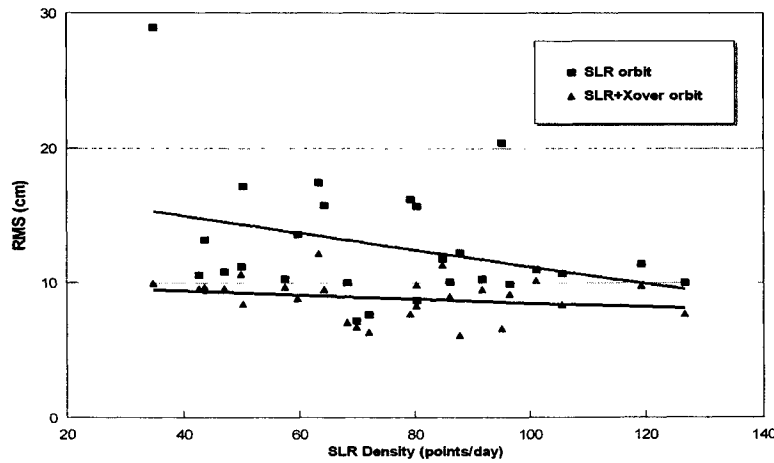


**Figure 8. GFO macro-model parameter sensitivity**  
*Uncorrelated Weighted Variance*

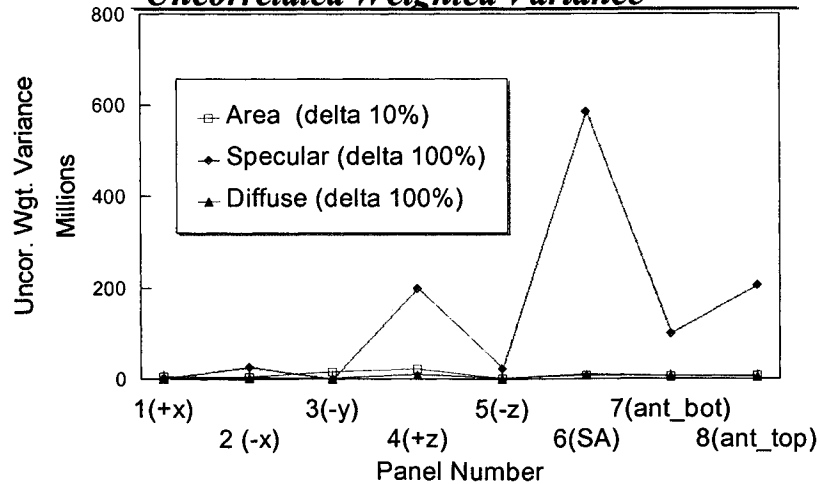


**Figure 9. Recovered Empirical Accelerations vary with Beta'**

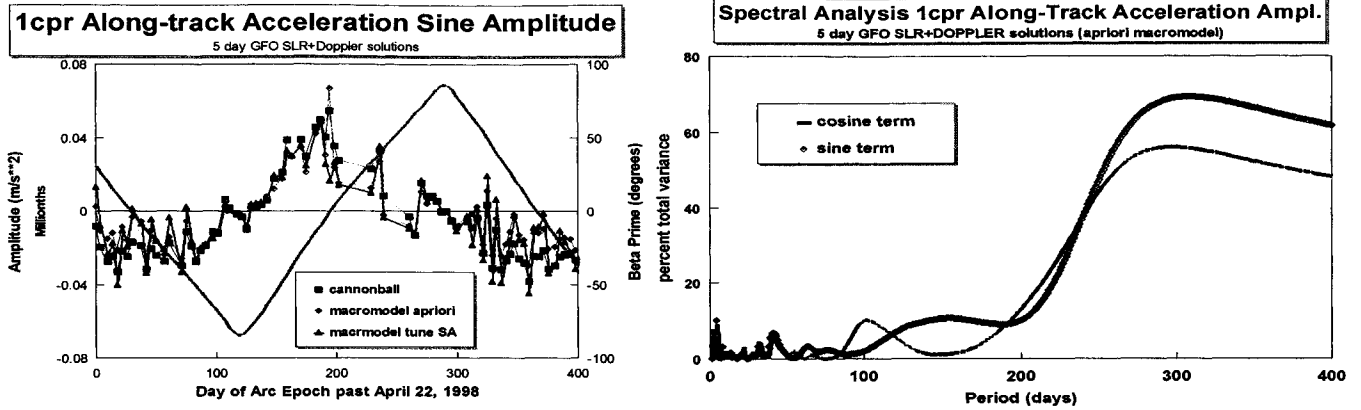


**Figure 10. Empirical Acceleration Amplitude and Phase retain strong Beta' signal**

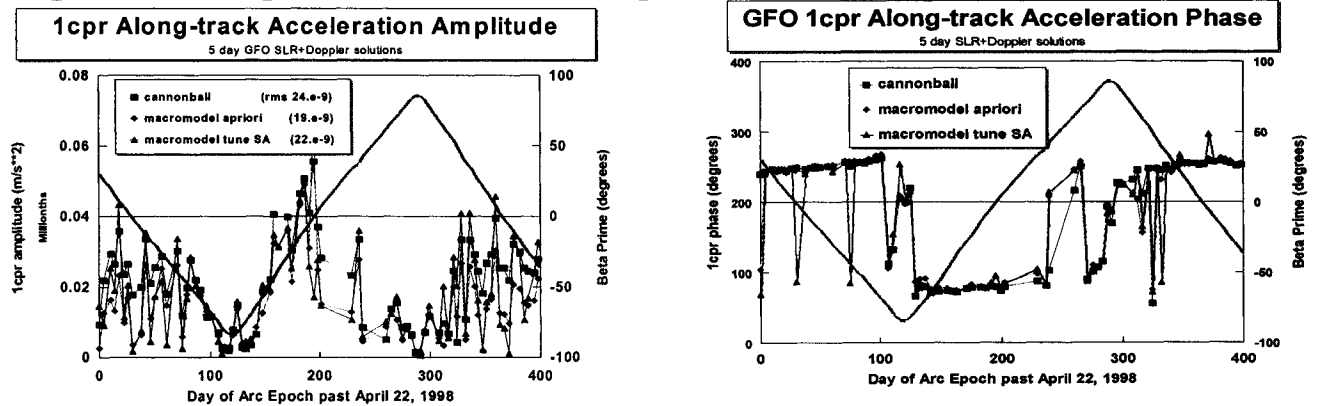


**Figure 11. GFO geographically projected orbit difference**

PGS7727 - PGS7609G radial orbit difference (cm)

PGS7727 - PGS7728 radial orbit difference (cm)

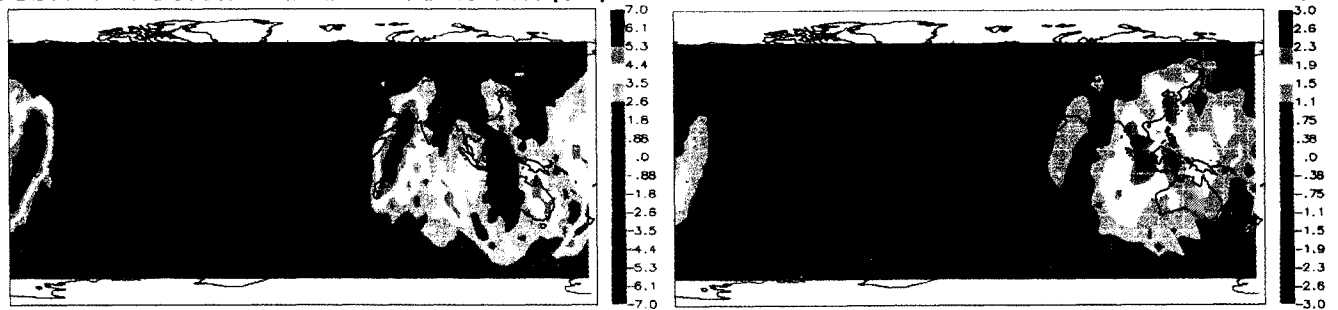
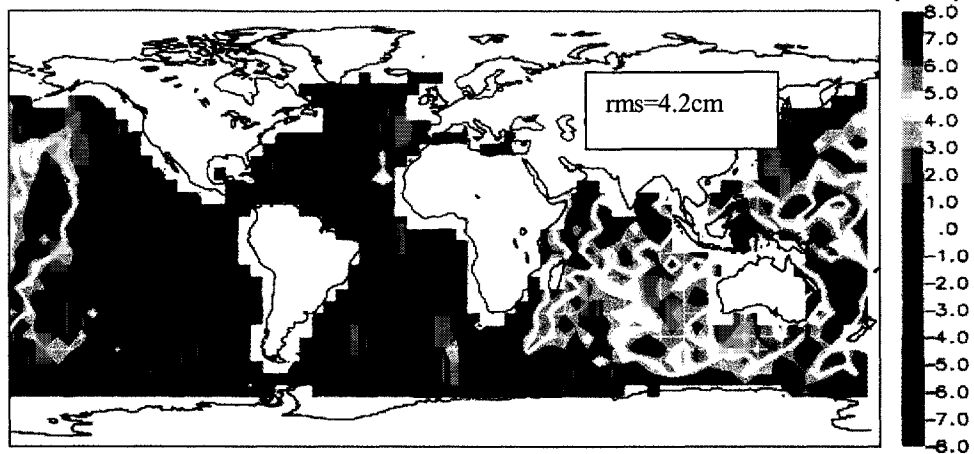
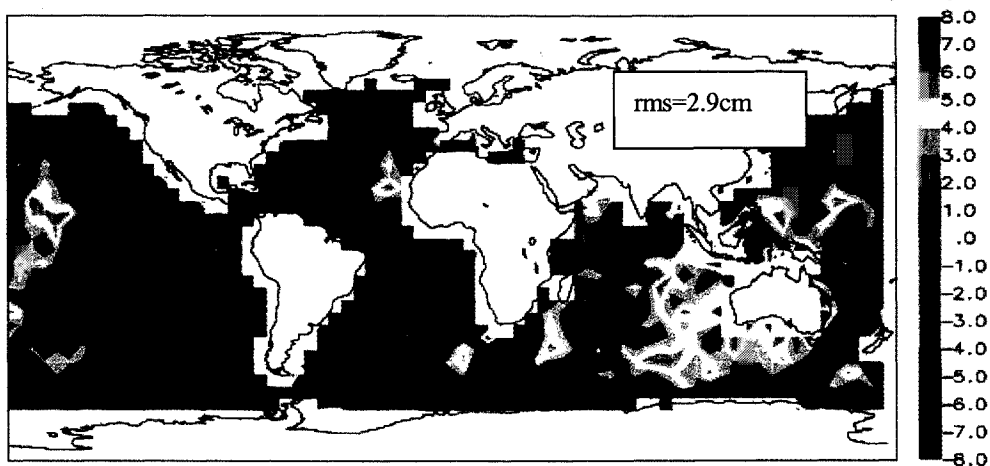


Figure 12. GFO geographically correlated orbit error

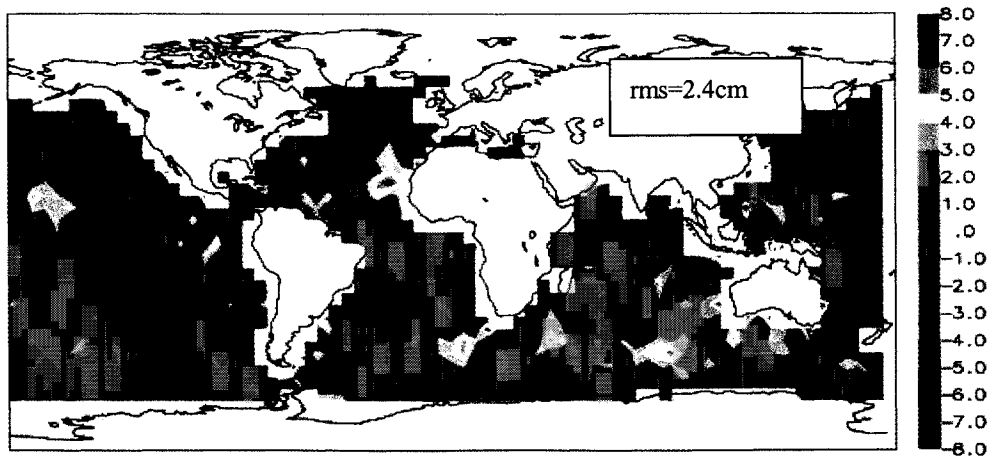
PGS7609G TOPEX-GFO altimeter crossover difference (cm)



PGS7728 TOPEX-GFO altimeter crossover difference (cm)



PGS7727 TOPEX-GFO altimeter crossover difference (cm)



## REFERENCES

1. Frazier W., Mitchell S., Weiss M., Wiener D., "Initialization and Early On-Orbit Performance of the Geosat Follow-On Satellite", *22nd AAS Guidance and Control Conference*, Feb '99, Breckenridge, Colorado, AAS 99-072.
2. Zelensky N.P., Luthcke S.B., Gehrman L., Rowlands D.D., Marshall J.A., Lemoine F.G., "Error Analysis of the GEOSAT Follow-On Satellite Orbit Determined Using SLR and GPS Tracking (abstract)," *Annales Geophysicae EGS XXII General Assembly*, Vol 15, suppl. 1, pp. C187, April 1997.
3. F.G. Lemoine, N.P. Zelensky, D.D. Rowlands, G.C. Marr, S.B. Luthcke, C.M. Cox, "Precise Orbit Determination for the GEOSAT Follow-On Spacecraft", 1999 Flight Mechanics Symposium Proceedings, NASA GSFC NASA/CP-1999-209235, pp. 495-507, May 1999
4. Pavlis, D.E., S. G. Poulou, S. C. Rowton, J. J. McCarthy, and S. B. Luthcke, GEODYN operations manuals, Raytheon ITSS contractor report, March 15, 2000.
5. F.G. Lemoine, S.C. Kenyon, J.K. Factor, R.G. Trimmer, N.K. Pavlis, D.S. Chinn, C.M. Cox, S.M. Klosko, M.H. Torrence, Y.M. Wang, R.G. Williamson, E.C. Pavlis, R.H. Rapp, and T.R. Olson, *The Development of the Joint NASA GSFC and NIMA Geopotential Model EGM96*, NASA/TP-1998-206861, July, 1998, NASA Goddard space Flight Center, Greenbelt, MD.
6. B.D. Tapley, C.K. Shum, J.C. Ries, S.R. Poole, P.A.M. Abusali, S.V. Bettadpur, R.J. Eanes, M.C. Kim, H.J. Rim, and B.E. Schutz, "The TEG-3 geopotential model," in *Gravity, Geoid, and Marine Geodesy* J. Segawa, H. Fujimoto, and S. Okubo (eds.), Vol 117, *International Association of Geodesy Symposia*, Springer-Verlag, Berlin, 453-460, 1997.
7. B.D. Tapley, M.M. Watkins, J.C. Ries, G.W. Davis, R.J. Eanes, R. Poole, H.J. Rim, B.E. Schutz, C.K. Shum, R.S. Nerem, F.J. Lerch, J.A. Marshall, S.M. Klosko, N.K. Pavlis, and R.G. Williamson, The Joint Gravity Model-3, *J. Geophys. Res.*, 101(B12), 28029-28049, 1996.
8. J.A. Marshall and S.B. Luthcke "Modeling Radiation Forces Acting on TOPEX/POSEIDON for Precision Orbit Determination," *Journal of Spacecraft and Rockets*, Vol 31, No. 1, 1994, pp. 99-105.
9. J.A. Marshall and S.B. Luthcke "Radiative Force Model Performance for TOPEX/POSEIDON for Precision Orbit Determination," *Journal of Astronomical Sciences*, Vol. 42, No. 2, 1994, pp. 229-246.
10. J.A. Marshall, N.P. Zelensky, S.M. Klosko, D.S. Chinn, S.B. Luthcke, K.E. Rachlin, R.G. Williamson, "The temporal and spatial characteristics of TOPEX/POSEIDON radial orbit error," *JGR*, Vol. 100, No. C12, pp. 25331-25252, Dec. 1995.
11. R. Scharroo, P. Visser, "Precise orbit determination and gravity field improvement for the ERS satellites," *J Geodhys. Res.*, vol 103, no. C4, pp 8113-8127, April 15, 1998.
12. Colombo, O.L., "Ephemeris errors of GPS satellites," *Bull. Geod.*, 60, 64-84, 1986.
13. Cretaux, J, F Nouel, C Valorge, P Janniere, "Introduction of emperical parameters deduced from the Hill's equations for satellite orbit determination," *Manuscripta Geod.*, 19, 135-156, 1994.
14. S.B. Luthcke, J.A. Marshall, S.C. Rowton, K.E. Rachlin, C.M. Cox, R.G. Williamson, "Enhanced Radiative Force Modeling of the Tracking and Data Relay satellites", *JAS* Vol. 45, No. 3, July-September 1997, pp. 349-370
15. F. J. Lerch, R. S. Nerem, D. .S. Chinn, J.C. Chann, G. B. Patel, and S. M. Klosko, "New error calibration tests for gravity models using subset solutions with independent data: Applied to GEM-T3," *Geophys. Res. Lett.*, 20(2), 249-252, 1993a.
16. D. D. Rowlands, S.B. Luthcke, J.A. Marshall, C.M. Cox, R.G. Williamson, S.C. Rowton "Space Shuttle Precision Orbit Determination in Support of SLA-1 Using TDRSS and GPS Tracking Data," *JAS* Vol. 45, No. 3, July-September 1997, pp. 349-370
17. Ray, R.D, "A Global Ocean Tide Model from TOPEX/POSEIDON Altimetry: GOT99.2," NASA/TM-1999-209478, NASA/GSFC Sep 1999.
18. Hedin, A.E., "The atmosphere model in the region 90 to 200 km," *Adv. Space Res.*, 8(5), 9-25, 1988